11 December 1998

ELSEVIER

Chemical Physics Letters 298 (1998) 227–232

CHEMICAL PHYSICS LETTERS

Fluorescence excitation spectrum of Ni–Ar complex

Yasunobu Kawamoto, Kenji Honma *

Department of Material Science, Himeji Institute of Technology, 1475-2 Kanaji, Kamigori, Hyogo 678-1297 Japan

Received 27 August 1998; in final form 28 September 1998

Abstract

A new absorption band is observed by a photolysis–supersonic jet experiment of nickelocene, $Ni(C_5H_5)_2$, at wavelengths near the Ni($y\,^1D_2$–$a\,^1D_2$) transition. This band appears only in the coexpansion of nickelocene with Ar or Ar in He. Taking into account dependencies of the band intensity on the photolysis laser power and nozzle pressure, this band is attributed to the transition of a Ni–Ar van der Waals complex. Since dispersed fluorescence of this band consists entirely of atomic transitions of Ni, the excited state of the Ni–Ar complex is considered to predissociate into $Ni^* + Ar$ with a very short lifetime. Analysis of the vibrational structure gives the excited-state binding energy $D'_0 = 51.7$ cm^{-1}. © 1998 Elsevier Science B.V. All rights reserved.

1. Introduction

We have studied the interactions of the first-row transition metal atoms with simple molecules and various important information has been accumulated [1–5]. However, the kinetic approach we have taken provides more or less qualitative information with respect to the interaction potentials, and dynamical or spectroscopic approaches are necessary to obtain detailed information about interaction potentials such as well depth, barrier height, occurrence of surface crossing, and so on. One alternative and useful technique to obtain such information is a spectroscopic study of low-temperature van der Waals complexes.

Laser-induced fluorescence and resonance-enhanced two-photon ionization techniques have been applied to metal atom–rare gas atom van der Waals complexes (M–Rg) and have provided much of the information about the interatomic potentials of M–Rg [6]. This powerful approach has been applied to metals in groups IA, IIA, IIB, and IIIA. The list of these kinds of studies has been extended to the noble metals, Cu [7], Ag [8,9], and Au [10]. In the complexes of these metals with rare gases, two band systems, $^2\Pi_{1/2,3/2}$–$^2\Sigma_{1/2}$, have been observed correlating to the $^2P_{1/2,3/2}$–^2S atomic asymptotes, and an additional band system correlating to the $^2D_{5/2}$–^2S asymptote has also been observed for Ag–Ar and Ag–Kr. Although these metals have d electrons, the electronic states of these atoms are rather simple because of the filled nd orbitals in the ground states.

Compared with the copper series, the other transition metals have much more complicated electronic structures, and there have been quite a few experimental studies for neutral van der Waals complexes containing transition metal atoms [11,12]. Recently, ab initio calculations have been carried out by Burda et al. for the interaction potentials of M–Xe, where M = Ni, Pd, and Pt [13]. In this Letter, we present a spectroscopic study of the van der Waals complex,

---

* Corresponding author. E-mail: honma@sci.himeji-tech.ac.jp

PII: S0009-2614(98)01178-6

Ni–Ar, which is the first experimental study of a complex between Ni and a rare gas.

2. Experimental

The experiment was carried out by using a supersonic jet–LIF apparatus which has been described previously [14]. Nickel atoms were generated by multi-photon dissociation of nickelocene at 266 nm. The nickelocene was issued through a pulsed nozzle (General Valve, 0.8 mm diam.) heated to 80°C. He, Ar, or their mixture was used as a carrier gas for the nozzle expansion. The fourth harmonic of a YAG laser (Continuum NY-82) was used to irradiate the nickelocene jet at $1-2$ mm downstream from the nozzle orifice to photolyze the molecules. The typical power of the 266 nm laser was 15 mJ/pulse. An $f = 1000$ mm lens was used but its focal point was about 100 mm away from the nickelocene jet. The output of a dye laser (Continuum ND-6000) pumped by another YAG laser was frequency doubled by a KD*P crystal to obtain radiation in the 300–310 nm region (Rhodamine 610). This tunable light was irradiated at 10–20 mm downstream from the photolysis laser. Laser-induced fluorescence was collected by a lens system and detected by a photomultiplier tube (Hamamatsu R-928). Dispersed fluorescence and excitation spectra were measured by using a monochromator (Nikon P-250). Nickelocene (95.0%) was obtained from Kanto Chem., and used without further purification. Helium (99.999%) and argon (99.999%) were obtained from Nihon Sanso.

3. Results and discussion

3.1. Laser-induced fluorescence

Fig. 1a shows the laser-induced fluorescence spectrum obtained by using Ar as a carrier gas. There are intense lines originating from the atomic transitions of Ni. Other than these atomic transitions, one band can be seen near the Ni($y\,^1D_2$–$a\,^1D_2$) transition, 301.29 nm (33190.9 cm^{-1}). In order to eliminate the contribution of atomic transitions, the excitation spectrum was measured by monitoring the emission at 310.25 nm which is the most intense peak in the dispersed fluorescence. The spectrum obtained is shown in Fig. 1b. Because the dispersed fluorescence consists of atomic transitions, as we will discuss in Section 3.2, some atomic peaks are not eliminated completely. However, the new band is isolated and its structure is clearly seen in this spectrum.

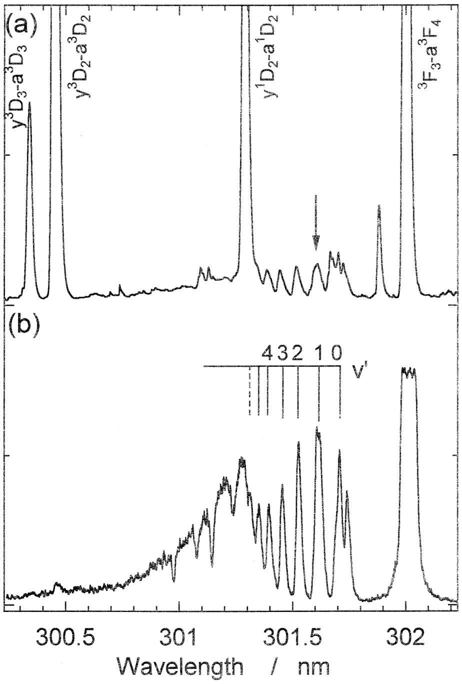

Fig. 1. Laser-induced fluorescence excitation spectrum obtained by a photolysis–jet expansion condition of nickelocene mixture in Ar. (a) Intensity of undispersed fluorescence was monitored. (b) Intensity of the emission at 310.25 nm, Ni($^3F_3$–$a\,^3D_2$), was monitored by a monochromator.

The LIF intensity of this band was measured as a function of the photolysis laser power. The intensity of the new band shows a quadratic dependence which is identical to the LIF intensity of the Ni($^3F_4$–$a\,^3F_4$) transition. The quadratic dependence is consistent with the two-photon dissociation of nickelocene to form the free nickel atom (Eq. (1)). [1]

$$\mathrm{Ni(C_5H_5)_2} + 2h\nu \rightarrow \mathrm{Ni} + 2\mathrm{C_5H_5}\,. \qquad (1)$$

That is, the new band originates from species containing single nickel atoms formed by the two-photon dissociation of nickelocene. Additional information was obtained from the measurement of the LIF

---

[1] The mean bond dissociation energy of Ni–C_5H_5 is 2.86 ± 0.30 eV, given by Ref. [15]. Two 266 nm photons are required to dissociate two Ni–C_5H_5 bonds.

intensity as a function of the nozzle pressure. The result shows that the new band appears at higher nozzle pressure than the ground-state Ni atom. This dependence suggests that the new band is attributed to a van der Waals complex. Since the photolysis occurs at 1–2 mm from the nozzle and the effect of the nozzle pressure would be more pronounced after the photolysis, the complex is more likely to be formed after the photolysis, i.e. the new band originates from a complex of the Ni atom. Taking into account the fact that only Ar or a mixture of Ar in He gives this band, it can be concluded that the new band is ascribed to a Ni–Ar$_n$ $(n \geqslant 1)$ complex. Although the number of Ar atoms in the complex is still an open question, the vibrational structure we will discuss below is consistent with a diatomic complex. Thus, we conclude that the new band is ascribed to an electronic transition of the Ni–Ar complex.

3.2. Dispersed fluorescence and dynamics of excited state

Dispersed fluorescence is expected to provide useful information about excited-state dynamics and the vibrational structure of the ground state. The dispersed fluorescence spectrum shown in Fig. 2 was measured by excitation at 301.59 nm indicated by an arrow in Fig. 1a. The excitation at other peaks and in the broad part of the band provides an almost identical spectrum. The spectrum does not have any of the vibrational structure expected for the emission corresponding to a bound–bound transition of the complex. Instead of the complex transition, all the peaks in this spectrum can be assigned to atomic transitions of Ni. Most of the intense peaks are assigned to transitions from Ni($^3F_3$) and there are some other transitions from Ni($^3F_{2,4}$, z $^1P_1$, z $^1D_2$) as indicated in Fig. 2. The absence of emission from the complex suggests that the excited state of Ni–Ar predissociates to Ni* + Ar with a very short lifetime. It may be reasonable to assume the fluorescence lifetime of the complex to be of the same order as those of the Ni atom, typically 10 ns [16]. If a detection limit of the complex fluorescence is assumed to be 1% of the atomic peaks, an upper limit of the lifetime is estimated to 0.1 ns. This limit is reasonable because the atomic emission following the complex excitation shows an identical time profile to the corresponding emission following atomic excitation.

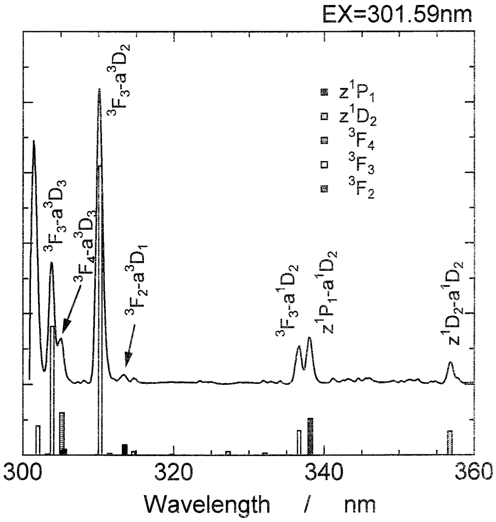

Fig. 2. Dispersed fluorescence spectrum obtained by excitation at 301.59 nm. The simulated spectrum is represented by a bar graph.

The predissociative nature of the excited state prevents us from obtaining potential information for the ground-state complex. However, another important piece of information, the product-state distribution, can be obtained by analyzing the intensities of the atomic peaks. By using the atomic transition probabilities tabulated by Fuhr et al. [16], the peak heights were reproduced as shown by the bar spectrum in Fig. 2. Relative yields of Ni* determined by this analysis are summarized in Table 1 with electronic energies [17]. Although there is no intense transitions from y ^3D_J in the wavelength region shown in Fig. 2, careful analysis of shorter wavelength region provides the yields of y $^3D_{2,3}$ listed in Table 1.

One possible mechanism for the predissociation is the spin–orbit predissociation via a repulsive surface. Funk and Breckenridge have observed the efficient formation of Cd($^3P_2$) + Xe by the excitation of the Cd–Xe complex correlating to Cd($^1P_1$) + Xe [18]. They have attributed the efficient predissociation to the surface crossing of the initially excited Cd–Xe(C $^1\Pi_1$) state with the repulsive c $^3\Sigma_1$ state, both having the same $\Omega = 1$. Although the more complicated electronic structure of the Ni atom makes a detailed analysis like that of Cd–Xe difficult, a

Table 1
Relative population of excited states formed by predissociation of the Ni–Ar complex

Term	Energy/cm^{-1} [a]	Relative population[b]
$\mathrm{y}\,^3\mathrm{D}_1$	34408.57	–[c]
$\mathrm{y}\,^3\mathrm{D}_2$	34163.29	0.03
$\mathrm{y}\,^3\mathrm{D}_3$	33500.85	0.03
$^3\mathrm{F}_2$	33610.92	0.03
$^3\mathrm{F}_3$	33112.37	1.00
$^3\mathrm{F}_4$	32973.41	0.15
$\mathrm{z}\,^1\mathrm{P}_1$	32982.28	0.06
$\mathrm{z}\,^1\mathrm{D}_2$	31441.67	0.09

[a] All data are taken from Ref. [13].
[b] All populations are given as the relative values to that of Ni($^3\mathrm{F}_3$).
[c] This level was not observed in the dispersed fluorescence.

similar mechanism is possible in the Ni–Ar complex. Some of the states developed from Ni* ($^3\mathrm{F}_{2,3,4}, \mathrm{z}\,^1\mathrm{P}_1, \mathrm{z}\,^1\mathrm{D}_2$) + Ar could be repulsive and cross with the upper state initially excited. Because the excitation of the $v' = 0$ vibronic level exclusively forms the excited states of Ni, the crossing must occur near the bottom of the upper-state potential surface.

3.3. Potential parameter of the excited state and atomic asymptote of the complex

The excitation spectrum (Fig. 1b) shows vibrational structure in which the spacing decreases at shorter wavelength and converges to a continuum. The binding energy is obtained by an extrapolation of the vibronic levels to the dissociation limit There are commonly used methods for the extrapolation of vibronic levels to determine dissociation energies, the Birge–Sponer (BS) analysis [19] and the LeRoy–Bernstein (LB) one [20,21]. A BS plot requires knowledge of the vibrational quantum numbers. In diatomic molecules, or complexes having isotopomers, the isotope shift of each peak provides a rigorous assignment of the vibrational quantum numbers. However, the Ni–Ar complex observed here shows line widths which are broader than the frequency shift for isotopmers. [2] Without the help of isotope shifts, one reasonable assignment could be made by studying the intensity change of vibrational peaks. The intensity changes smoothly toward lower energy and a sharp drop without any peak can be seen after the lowest energy peak. Therefore, we assigned the lowest energy peak as $v' = 0$ of the excited state. The vibrational quantum number determined by this manner is shown in Fig. 1b and the frequencies of vibrational peaks are summarized in Table 2. The BS plot of this series is shown in Fig. 3a, which shows a linear relation within the experimental error. The ω_e and $\omega_e x_e$ values were determined to be 12.4 and 0.73 cm^{-1}, respectively. A linear extrapolation of this plot provides the dissociation limit and the dissociation energy of the excited state to be 33193 cm^{-1} and $D_0 = 46.5$ cm^{-1}, respectively.

In the LB analysis, the level spacing is described by a power law, $(\Delta G_v)^n \propto D_0 - E_\mathrm{v}$, where $\Delta G_v = [E(v+1) - E(v-1)]/2$, D_0 is the dissociation energy and E_v is the total vibrational energy of the state. For a van der Waals interaction, 3/2 is used as the exponent. The LB plot for Ni–Ar is shown in Fig. 3b, and the dissociation limit determined by this plot is 33198 cm^{-1}. The binding energy can be obtained as the difference between this dissociation limit and the lowest energy vibrational level observed, $D_0 = 51.7$ cm^{-1}. The dissociation limit obtained from the LB analysis is slightly larger than that from the BS analysis. The LB analysis is appropriate if levels at the convergence limit are measured, whereas the BS one may not be adequate for weakly interacting systems. Here, we observed the level up to 7.5 cm^{-1} lower than the dissociation limit. Thus, we take the values determined from the

Table 2
Assignments and transition frequencies of Ni–Ar

$v' - v''$	ν_obs/cm^{-1}
0–0	33146.3
1–0	33157.6
2–0	33166.7
3–0	33174.7
4–0	33181.4
5–0	33186.2
6–0	33190.5

---

[2] The isotope shift of a given v is given by $\Delta\nu = (1-\rho)\omega_e(v+1/2) - (1-\rho^2)\omega_e x_e(v+1/2)^2$. For the ω_e and $\omega_e x_e$ values determined below, the shift between $^{58}\mathrm{Ni}^{40}$ Ar and $^{60}\mathrm{Ni}^{40}\mathrm{Ar}$ has a maximum value, 0.37 cm^{-1}, at $v = 4$.

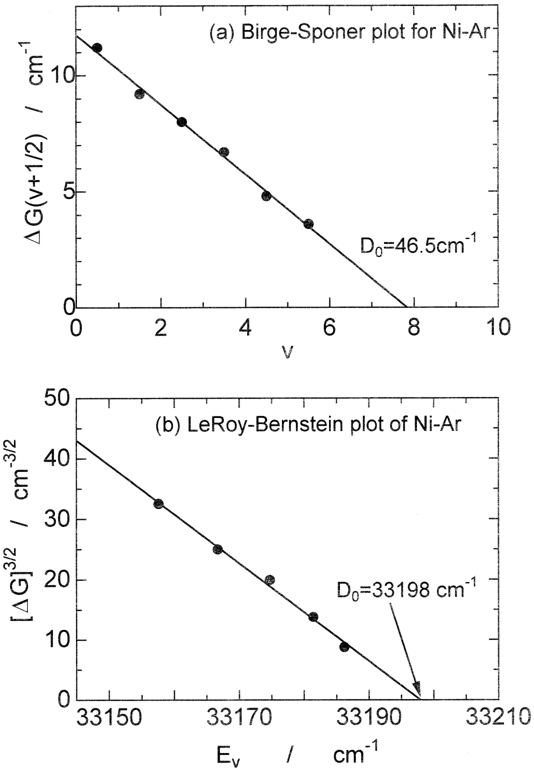

Fig. 3. (a) The BS plot for the vibronic structure of the Ni–Ar complex. (b) The LB plot for the same vibronic structure.

LB analysis, i.e. 33198 cm^{-1} for the dissociation limit and 51.7 cm^{-1} for the dissociation energy.

It is better to note that the above analysis is based on a single electronic transition. More than two electronic states for the Ni–Ar complex can be developed from any atomic asymptotes because of their non-zero J values. Thus, it may be possible that more than two transitions are lying close together in the present energy region. Although higher resolution may resolve them, the vibronic structure observed here is consistent with a single electronic transition except for the splitting of the $v = 0$ level.

One open question in the Ni–Ar complex is the assignment of atomic asymptotes for the lower and upper states of the observed transition. For discussion, the energy levels of the Ni atom are summarized in Fig. 4. The listed excited states are accessible from the lowest-lying states by the transition of the wavelength region studied here. For the asymptote of the upper state, useful information is obtained by analyzing the dispersed fluorescence. The highest energy level observed in the dispersed fluorescence is Ni(y$\,^3$D$_2$) for the excitation of the discrete peaks. This provides the lower limit for the $v' = 0$ level of the upper state. Since a reasonable upper limit can be selected to be Ni(y$\,^1$D$_2$), which is the highest level accessible from Ni(a$\,^1$D$_2$) in the wavelength region studied here, there are three possibilities for the atomic asymptote of the upper state, i.e. y$\,^1$D$_2$, y$\,^1$F$_3$, and y$\,^3$D$_1$. Although no direct evidence is available to determine which of three it is, it may be useful to evaluate the binding energy of the lower state. By using the dissociation limit of the upper state, 33198 cm^{-1}, the binding energy of the lower state can be calculated by $D''_0 = 33198 - [E_u - E_l]$, where E_u and E_l are the energies of upper and lower atomic asymptotes, respectively. For three candidates, y^1D_2,y$\,^1$F$_3$, and y$\,^3$D$_1$, E_u = 36600.81, 35639.15, and 34408.57 cm^{-1}, respectively. Because D''_0 must be

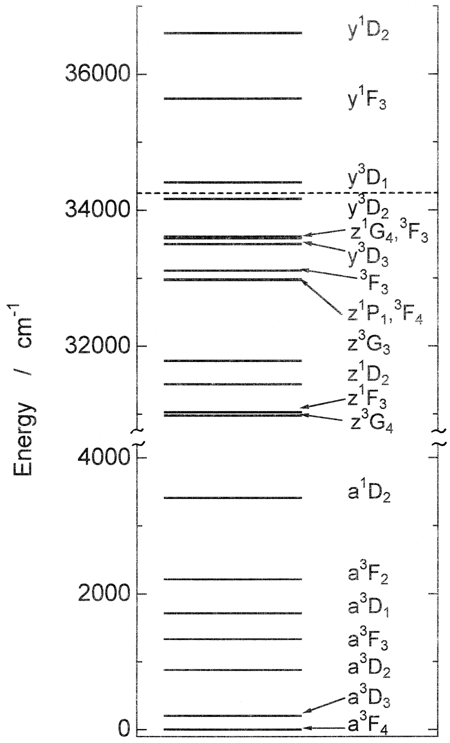

Fig. 4. Level energy diagram of Ni. The lowest lying three states, seven levels, and excited states relevant to this study are summarized. All energies are taken from Ref. [13]. The broken line indicates the lower limit of the $v = 0$ level of the complex.

positive, lower limits of E_1 are given as 3403,2441, and 1211 cm^{-1}, for y $^1D_2$, y $^1F_3$, and y $^3D_1$, respectively. Thus, possible upper–lower asymptotes and the binding energies of lower states are y $^1D_2$–a $^1D_2$ (7 cm^{-1}), y $^1F_3$–a $^1D_2$ (969 cm^{-1}), y $^3D_1$–a $^1D_2$ (2199 cm^{-1}), y $^3D_1$–a $^3F_2$ (1006 cm^{-1}), y $^3D_1$–a $^3F_3$ (121 cm^{-1}), and y $^3D_1$–a $^3D_1$ (502 cm^{-1}). Because of the repulsive nature of the $4s^2$ configuration, a $^3F_3$ and a $^3F_2$ are less likely than a $^1D_2$ or a $^3D_1$. Among the four candidates, the binding energies 2199 and 969 cm^{-1} could be unfavorable because they are much larger than the binding energies of noble metal–rare gas complexes [3–6]. The 502 cm^{-1} binding energy may be still large compared with the binding energy of noble metal–rare gas complexes because both Ni(a $^3D_1$) and the ground states of noble metals have the same ns^1 configuration. Although 7 cm^{-1} may not be surprisingly small, if we consider the theoretical study that predicted no bound state in the Ni–Xe complex where the dispersion interaction must be larger than Ni–Ar [8], it may be too small for the observation under our experimental conditions. Hence, it is still difficult to decide which is the most probable asymptote for the lower state, and more theoretical study is required.

4. Conclusion

The laser-induced fluorescence excitation spectrum was observed for the Ni–Ar van der Waals complex. The absorption band shows vibronic structure which was analyzed to obtain the dissociation limit of the complex. The binding energy of the upper electronic state was determined to be 51.7 cm^{-1}. The dispersed fluorescence consists entirely of the atomic emission of Ni^* which suggests that the upper state of the complex predissociates to $Ni^* + Ar$ with a short lifetime. Since all vibronic peaks show almost identical spectra, the predissociation occurs via surface crossing with a dissociative state near the bottom of the upper state. Conclusive assignment of the atomic asymptotes could not be made for the lower and upper states of the complex, and more theoretical studies are required.

References

[1] D.E. Clemmer, K. Honma, I. Koyano, J. Phys. Chem. 97 (1993) 11480.
[2] K. Honma, M. Nakamura, D.E. Clemmer, I. Koyano, J. Phys. Chem. 98 (1994) 13286.
[3] K. Senba, R. Matsui, K. Honma, J. Phys. Chem. 99 (1995) 13992.
[4] R. Matsui, K. Senba, K. Honma, J. Phys. Chem. 101 (1997) 179.
[5] C.L. Haynes, K. Honma, J. Chem. Soc. Faraday Trans. 94 (1998) 1171.
[6] See for example W.H. Breckenridge, C. Jouvet, B. Soep, in: M.A. Duncan (Ed.), Advances in Metal and Semiconductor Clusters, vol. III, JAI Press, Greenwich, CT, 1995.
[7] L.R. Brock, M.A. Duncan, Chem. Phys. Lett. 247 (1995) 18.
[8] C. Jouvet, C. Lardeux-Dedonder, S. Martrenchard, D. Solgadi, J. Chem. Phys. 94 (1991) 1759.
[9] L.R. Brock, M.A. Duncan, J. Chem. Phys. 103 (1995) 9200.
[10] A.M. Knight, A. Stangassinger, M.A. Duncan, Chem. Phys. Lett. 273 (1997) 265.
[11] H. Wu, L.-S. Wang, J. Chem. Phys. 107 (1997) 16.
[12] H. Wu, S.R. Desai, L.-S. Wang, J. Chem. Phys. 103 (1995) 4363.
[13] J.V. Burda, N. Runeberg, P. Pyykko, Chem. Phys. Lett. 288 (1998) 635.
[14] K. Honma, J. Chem. Phys. 99 (1993) 7677.
[15] S. Leutwyler, U. Even, J. Jortner, Chem. Phys. 58 (1981) 409.
[16] J.R. Fuhr, G.A. Martin, W.L. Wiese, J. Phys. Chem. Ref. Data 17 (1988) Suppl. 4.
[17] J. Sugar, C. Corliss, J. Phys. Chem. Ref. Data 14 (1985) Suppl. 2.
[18] D.J. Funk, W.H. Breckenridge, J. Chem. Phys. 90 (1989) 2927.
[19] G. Herzberg, Molecular Spectra and Molecular Structure I. Spectra of Diatomic Molecules, Van Nostrand Reinhold, New York, 1950.
[20] R.J. Le Roy, R.B. Bernstein, J. Chem. Phys. 52 (1970) 3869.
[21] R.J. Le Roy, R.B. Bernstein, J. Mol. Spectrosc. 37 (1971) 10920.